

PROCEEDINGS OF SPIE

SPIDigitalLibrary.org/conference-proceedings-of-spie

Portable LWIR hyperspectral imager based on MEMS Fabry-Perot interferometer and broadband microbolometric detector array

David Béland, Hélène Spisser, Denis Dufour, Loïc Le Noc, Francis Picard, et al.

David Béland, Hélène Spisser, Denis Dufour, Loïc Le Noc, Francis Picard, Patrice Topart, "Portable LWIR hyperspectral imager based on MEMS Fabry-Perot interferometer and broadband microbolometric detector array," Proc. SPIE 10545, MOEMS and Miniaturized Systems XVII, 105450S (22 February 2018); doi: 10.1117/12.2291751

SPIE.

Event: SPIE OPTO, 2018, San Francisco, California, United States

Portable LWIR hyperspectral imager based on a MEMS Fabry-Pérot interferometer and a broadband microbolometric detector array

David Béland*, H el ene Spisser, Denis Dufour, Lo ic Le Noc, Francis Picard and Patrice Topart
INO, 2740 Einstein Street, Quebec, Quebec, Canada, G2P 4S4

ABSTRACT

The fast growing consumer electronics market of connected and wearable devices is driving a wealth of new applications. Personal capability for detecting and monitoring substances part of our everyday life (food, cosmetics, drugs, etc.) by spectroscopic means will soon become a reality as a number of new miniature spectrometers are being reported. These devices mostly operate in the visible and near infrared spectral region due to the readily available low-cost detectors in these spectral regions. However, enhanced selectivity is achievable in the molecular fingerprint spectral region (7-20 μm), allowing for applications that would be difficult or impossible at lower spectral wavelengths. To this end, a compact, portable, Long-Wave Infrared (LWIR) hyperspectral imager was developed. It is based on INO's MICROXCAM-384 camera featuring a 384 x 288 pixel, 35 μm pitch uncooled bolometric broadband Focal Plane Array (FPA) and Fraunhofer ENAS' 2 mm x 2 mm aperture MEMS tunable Fabry-P erot Interferometer (FPI). The INO's broadband FPA exhibits a Noise Equivalent Temperature Difference (NETD) lower than 25 mK (for the 8-12 μm range at 300 K, 50 fps and $f/1$) and a flat spectral response from 3 to 14 μm . The footprint of the hyperspectral imager is 7 cm x 8 cm x 10 cm excluding the source. The spectral resolution varies from 55 to 220 nm depending on the type of FPI used. The Noise Equivalent Spectral Radiance (NESR) is 430 $\text{mW}/(\text{m}^2 \cdot \text{sr} \cdot \mu\text{m})$ at 9 μm . Using this hyperspectral imager, spectra of various substances including polymers were recorded in the transmission, reflection and transmittance configurations. A good agreement was found with spectra obtained by applying the FPI transfer function to spectra recorded with a commercial FTIR spectrometer. The LWIR configuration of the imaging spectrometer will be described and test results presented.

Keywords: Hyperspectral imaging, Mid-IR imaging, microbolometer, MEMS Fabry-P erot, nondestructive testing, chemical compounds analysis, spectroscopy

1. INTRODUCTION

The world of spectroscopy is currently undergoing a revolution due to the convergence of several microelectromechanical systems (MEMS) based technologies. The integration of MEMS microbolometer arrays with MEMS scanning Fabry-P erot interferometers (FPI) and miniaturised imaging lenses are enabling the creation of small, low-cost hyperspectral imaging instruments that can work in the infrared "Molecular Fingerprint" region of the electromagnetic spectrum. In this spectral region, spanning approximately the 600 to 1400 cm^{-1} (7 to 20 μm) range, the absorption spectra from organic molecules exhibit unique, complex overlapping shapes due to their stretching and bending modes, allowing for the enhanced selectivity of specific constituents of complex mixtures. Until now, fingerprint region spectroscopy has mostly been achieved using large, expensive Fourier Transform Interferometer (FTIR) based instrumentation. These instruments are typically confined to laboratory environments and operated by trained specialists. The emergence of smaller, low-cost imaging spectrometers will greatly diminish the barrier of entry for infrared spectroscopy and lead to widespread adoption outside the laboratory. Subsequently, the development of a host of new applications is envisioned in fields such as agriculture and food quality, advanced manufacturing, biomedical and security. Emerging miniaturised spectral imaging technologies could also eventually lead to new consumer applications for smartphones, wearables and Internet of Things (IoT) devices.

To this end, INO has developed a portable fingerprint region hyperspectral imager, the MICROXCAM-384i-HS platform, intended for customers who wish to develop new applications inside and outside the laboratory.

A development kit has also been created which includes driver electronics and data acquisition software to ease the use of the device. This paper focuses on the key specifications of the newly developed camera along with performance test results and images obtained in the LWIR spectral region.

2. SYSTEM DESCRIPTION

2.1 MICROXCAM-384i-HS Overview

Building on its strengths in microbolometer sensor technology [1], INO has developed a compact hyperspectral imaging camera specifically designed for the infrared fingerprint region. This instrument, MICROXCAM-384i-HS, is shown in figure 1. It is based on the 384 x 288, 35 μm pitch uncooled microbolometer detector that has been used by INO over the last several years in many of its infrared and Terahertz band cameras [2]. Recently, INO developed a gold black deposition process for its 384 x 288 FPA, enabling high sensitivity imaging over an unprecedented wavelength range from 2 μm to Terahertz [3]. This sensor is connected to an INO MICROXCAM camera core, a recently-developed update to INO's IRXCAM camera core that provides a smaller, lighter camera system [4]. The MICROXCAM camera interfaces the data acquisition and control computer by an Ethernet link. The camera is controlled and configured using INO's proprietary software.

This microbolometer sensor is coupled to a MEMS scanning FPI and a miniature imaging lens to enable spectral imaging over the allowable spectral range defined by the specific FPI used. The FPI plus the lens assembly is a modular add-on, shown as the black component attached to the front of the grey-colored MICROXCAM camera core. The FPI plus lens module can be easily changed for another one, allowing measurements for a different spectral range while keeping the same infrared sensor and camera core. The baseline LWIR configuration, designed for fingerprint region spectroscopy, covers a spectral range of 8 to 11 μm , with a spectral resolution ranging from 130 nm at 8 μm to 220 nm at 11 μm . We measured a Noise Equivalent Spectral Radiance (NESR) of 430 $\text{mW}/(\text{m}^2 \cdot \text{sr} \cdot \mu\text{m})$ at 9 μm . The NESR refers to the sensor noise in term of spectral radiance units. Given the fact that the FPI transmission wavelength is tunable, the system can either be used as a random-access, multispectral imager or the FPI can be scanned to allow hyperspectral imaging, with center wavelength precision of 10nm. The acquisition time per spectral sample is currently 0.18 s and will soon decrease with the future development of enhanced custom electronics for FPI image acquisition synchronization. The FPI aperture of 2 x 2 mm reduces the region of interest on the 384 x 288 FPA to 100 x 100 pixels. Different FPI modules operating at lower wavelengths, from 3.8 μm to 5.3 μm for example are also currently available. If required by a particular application, it is also possible to custom-fabricate FPIs for other infrared spectral ranges within the 3 to 14 μm range.

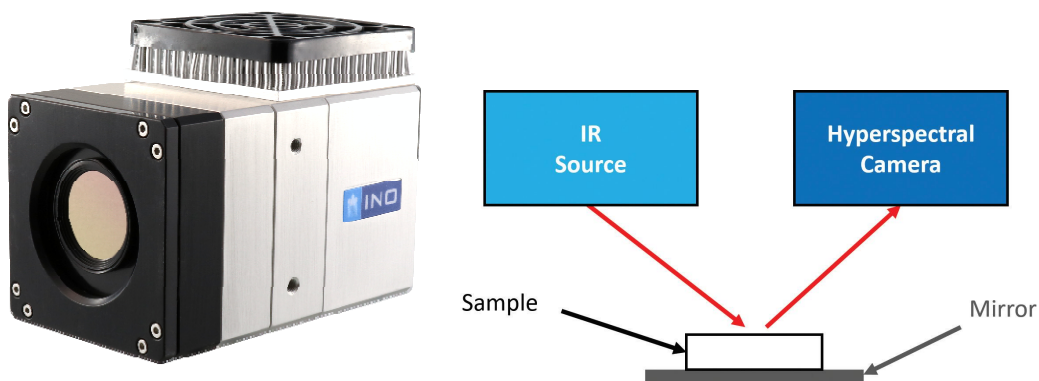


Figure 1. Left: INO's MICROXCAM-384i-HS spectral imaging camera. The front part in black color is the interferometer-lens module. The grey part includes the FPA module with the camera control electronics; Right: Development kit camera-source-sample configuration for reflectance mode spectral imaging measurements.

INO has devised a development kit platform for the MICROXCAM-384i-HS imaging spectrometer, to facilitate the development and testing of infrared hyperspectral imaging applications by end-users. In addition to the spectral imaging camera, the development kit includes an optional infrared source and sample holder designed to allow users to perform reflectance-mode spectral imaging measurements. In the proposed development kit configuration, a broadband infrared source provides illumination over a 1.5 inch diameter sampling area. With the camera at a distance of 80 mm from the sample, the image of this sampling area is spread over 40 FPA pixels, each pixel corresponding to a 0.9 mm spatial resolution at the sample. Hence, the system can acquire “macro”-size spectral images, unlike the small sample imaging areas currently provided by imaging FTIR systems. This could prove very useful in applications such as impurity detection. Under typical operating conditions, a Signal to Noise Ratio (SNR) of 2800 is achieved with this system. MICROXCAM-384i-HS is ready for acquisition 2 minutes after turning it on. Temperature stabilization is achieved by the active internal temperature control of both the interferometer and FPA modules. The LabVIEW-based, user friendly software allows visualization of images and spectra at selected locations. Spectral measurement datacubes are saved in a user-friendly text file format, allowing them to be easily imported by a spectral analysis software. The specifications of MICROXCAM-384i-HS discussed above are summarized in Table 1 below.

Table 1. MICROXCAM-384i-HS specifications

Technical Specifications	
Spectral Range	8-11 μm
Spectral Resolution	130 nm at 8 μm 220 nm at 11 μm
Acquisition Time	0.18 s per wavelength sample < 3 min (full spectral range, 25 nm sampling)
Field of View	$\pm 41^\circ$ (100 pixel diameter image)
Supply	24 V _{DC} nominal, < 7W typical
Dimensions	61 mm (H) x 78.5 mm (W) x 101 mm (L)
Weight	420g

2.2 Microbolometer Detector Array

In comparison with the cooled infrared imaging arrays used in FTIR instruments, microbolometer sensors are uncooled, small and inexpensive, making them an ideal choice for miniaturised, low-cost infrared spectral imaging systems. Furthermore, INO has developed a process for deposition of a gold-black broadband absorber over the microbolometer array’s pixels. The gold black absorber enhances the bolometer’s absorbance, and hence its sensitivity, by a factor of 2 in the LWIR band in comparison with INO’s standard bolometer absorbance. The gold-black absorber also allows for an extremely large wavelength absorption range from the visible to the Terahertz region of the electromagnetic spectrum. The FPA is thermally stabilized by a Thermoelectric Cooler (TEC).

Table 2. INO’s 384x288 microbolometer FPA key specifications

Technical Specifications	
Detector Pitch	35 μm
FPA Format	384 x 288
Detector Thermal Time Constant	22 ms
NETD	25 mK typical
Spectral Range	3-14 μm
Pixel Operability	> 99.8%

The methodology used to measure the NETD has been described in a previous paper [5]. In that work, the NETD was characterized for scene temperatures ranging between 20°C and 40°C. The following measurement parameters were

used: broadband AR-coated Ge window (3 to 14 μm wavelength), integration time of 40 μs , f-number of f/1, FPA temperature of 25°C and frame rate of 50 Hz. The estimated error on NETD measurement is 5%.

The spectral responsivity over the wavelength range from 3 to 14 μm was measured with a McPherson 205f monochromator. Its relative output irradiance was measured with two independent reference detectors, namely a pyroelectric detector and an InGaAs detector. The reference detector aperture was overfilled using appropriate optical elements, and the power density was deduced from the nominal detector area. During the measurements, the monochromator source lamp was modulated to greatly reduce the contribution from the radiative environment and emission from the optics (lens, grating). The output of the reference detectors was demodulated by a digital lock-in amplifier and logged by a data acquisition software. The spectral resolution of the monochromator source was set to 50 nm.

Following the power density measurement, two packaged FPAs were connected to INO's MICROXCAM electronics and exposed to the same modulated monochromatic source. The signal within the region of interest was averaged for each frame and demodulated by an algorithm. The responsivity was computed by dividing the resulting signal by the power spectral density. Figure 2 shows the relative detectivity thus obtained. For wavelengths below 8 μm , the sensitivity is more than 5 times higher for the new INO 384 x 288 FPA with gold black.

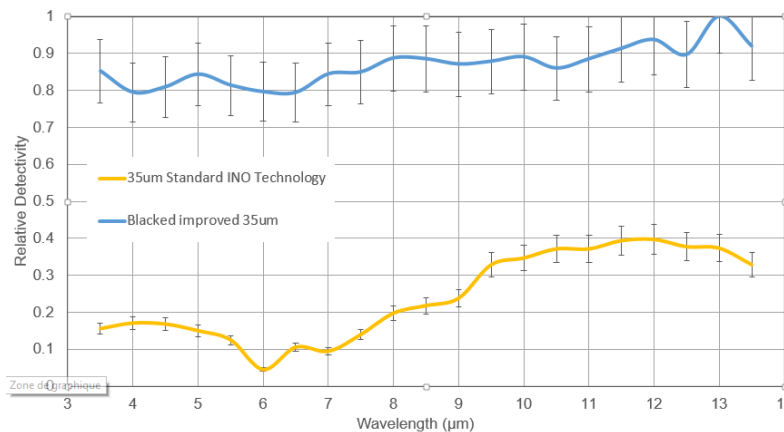


Figure 2. Detectivity of packaged FPAs from 3.5 to 13.5 μm [3].

2.3 Mid-IR Interferometer

The MEMS FPI implemented in the system is built by the Fraunhofer Institute for Electronic Nano Systems, ENAS, (Chemnitz, Germany). This micromachined interferometer presents an aperture of 2 mm x 2 mm. It is fully tunable through a spectral range from 8 to 11 μm by adjusting the resonator length by means of electrostatic actuation [6]. The response time constant of the FPI is 1 ms. The graph on the left-hand side of figure 3 shows transmission measurements performed with a Bruker FTIR spectrometer for calibrating the FPI first order resonance wavelength as a function of the applied actuation voltage. Compact and offering a good solution in terms of optical throughput, this technology is well suited for miniaturized and cost effective infrared imaging spectroscopy. The temperature of the device is actively controlled by the camera to ensure its calibration is maintained over time.

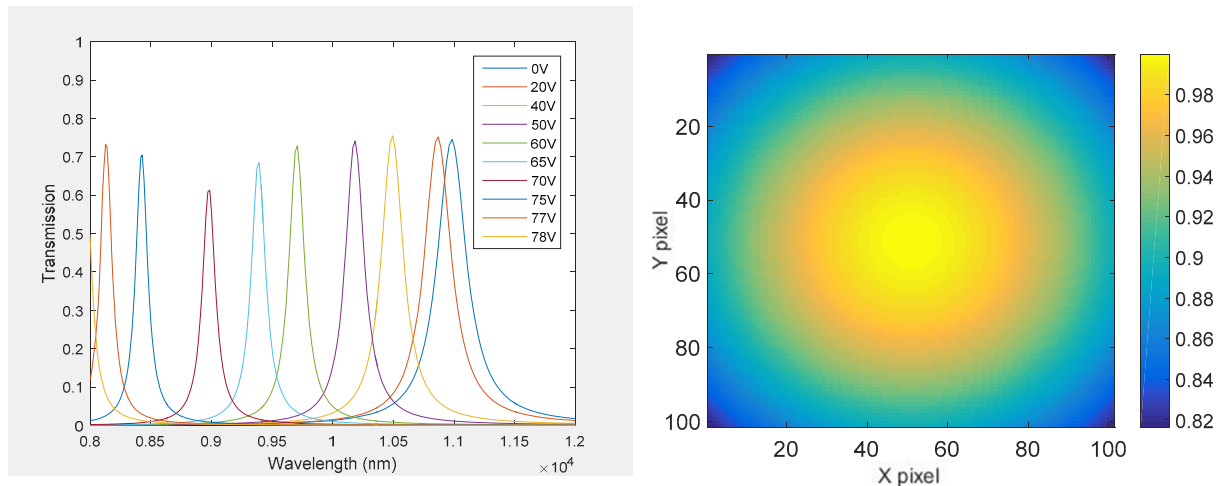


Figure 3. Left: Transmittance spectra of the filter's first order for various actuation voltages. Right: Multiplicative factor for wavelength correction.

The first-order resonance wavelength of the FPI varies with the light incident angle on the FPI. While imaging, this phenomenon implies a gradient in the maximum transmission wavelength seen by each pixel around the optical axis. The right-hand side of Figure 3 shows the correction factor that has to be applied to the center pixel's maximum transmission wavelength to obtain the maximum transmission wavelength for the other pixels in the camera image. This correction is applied when processing the hyperspectral datacube.

2.4 Data acquisition, processing and datacube construction

The complete MICROXCAM-384i-HS system comprises the elements presented in Figure 4. The data acquisition system gives the platform the ability to acquire a datacube at a rate of 0.18 s per spectral sample. In scanning mode, a 100 pixel x 100 pixel x 120 wavelength datacube (25 nm spectral sampling from 8 to 11 μm) is acquired in 22.5 s.

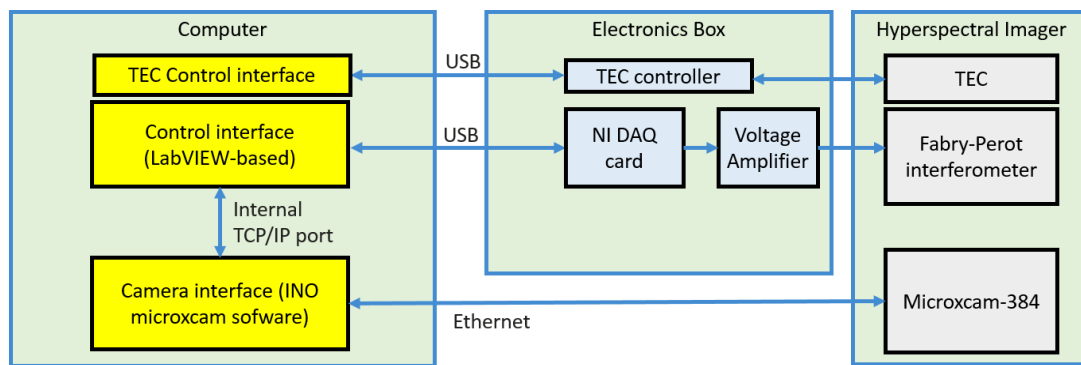


Figure 4. MICROXCAM-384i-HS block diagram

Three software applications running simultaneously in a Microsoft Windows 10 environment allow for the acquisition of the hyperspectral datacube. First, the MICROXCAM camera interface software controls the microbolometers FPA parameters and its readout electronics via an Ethernet connection. Image acquisition runs at a steady state of 50 fps. A second application is used to actively monitor and control the thermal environment around the interferometer by means of a TEC and associated temperature sensor. The third software application, illustrated below in Figure 5, is a LabVIEW developed application, having three principal functions. First, it synchronizes the analog output of the National

Instruments DAQ card driving the interferometer with the MICROXCAM image frame acquisition. Second, it processes the data to build the datacube and stores them on the computer. Its final function is to provide a user-friendly interface to control measurements, to give real-time feedback on the system status to the operator and to offer hyperspectral image and spectrum displays. Linked to a computer with two USB cables, the DAQ card, the voltage amplifier and the interferometer module TEC controller are assembled inside a 237 mm x 156 mm x 80 mm aluminum box, powered by a 24 V power supply. The interferometer module is connected to this controller box which supplies the FPI actuation voltages and TEC control.

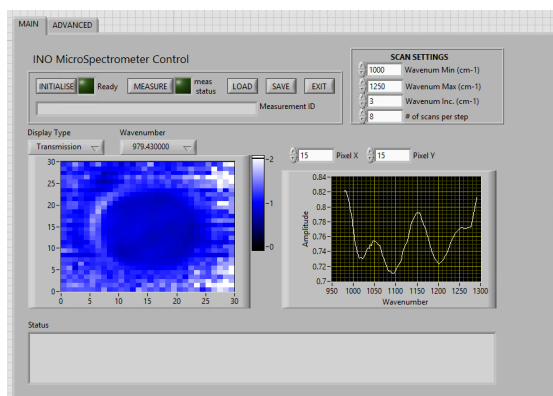


Figure 5. LabVIEW control software interface

3. PERFORMANCE

3.1 Imaging capabilities

The FPI aperture reduces the region of interest within the microbolometers FPA to a 100 pixel diameter area. With a $\pm 41^\circ$ field of view, a spatial resolution of 0.9 mm/pixel for an object at 80 mm from the camera is measured. The focus of the lens is a fixed parameter, allowing imaging from 40 mm to infinity. Test images of a blackbody source at 373K and a 4-bar calibration target are shown in Figure 6. The Modulation Transfer Function (MTF) was measured. The 50% MTF modulation level was found to correspond to a spatial frequency of 3.46 cycles/mm in the image plane.

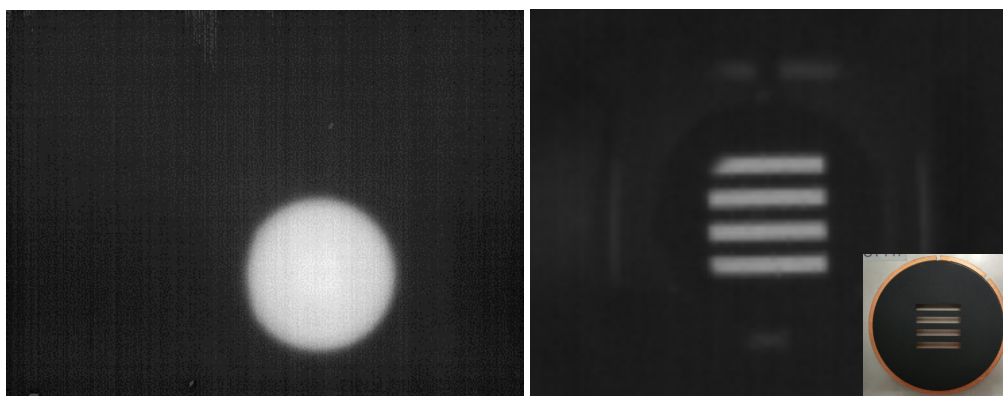


Figure 6. MICROXCAM-384i-HS imaging capabilities. Left: Spectral image at 9 μm of a blackbody source covering the field of view. Right: Zoomed image, of a 4-bars target with 2 mm x 18 mm rectangular slits placed in front of the blackbody source, at a distance of 100 mm from the camera.

3.2 SNR and calibration results

To perform a hyperspectral image measurement, a reference spectral image of an IR reflective mirror is first obtained, then the sample to test is placed over the mirror and a second spectral image is taken. The sample's relative spectral reflectance is then given by the ratio between the sample signal and the reference signal for each wavelength of the spectrum and each pixel included in the image. When the sample is not totally reflective, and partially transparent in the infrared, the method is called transreflectance since the signal passes twice through the sample, before and after reflection from the mirror. The total time to complete a measurement depends on the number of spectral points that are to be scanned and how much averaging by oversampling is performed. A typical total measurement time is less than 3 minutes.

The 100% line measurement is a method used to quantify the SNR and stability on the spectral dimension of the datacube, including all noise sources of the system. It consists of computing the ratio of two measurements of a gold IR reflective mirror, which normally gives a nominal transreflection ratio of 1. The ratio of 1 over the standard deviation of the raw signal of each pixel relates to the datacube spectral dimension SNR. The results shown on the right-hand side of Figure 7 give a SNR of 2830 over a span of 500 nm, and of 1280 over the full spectral range. The source used is a 1 inch blackbody cavity at 1273K.

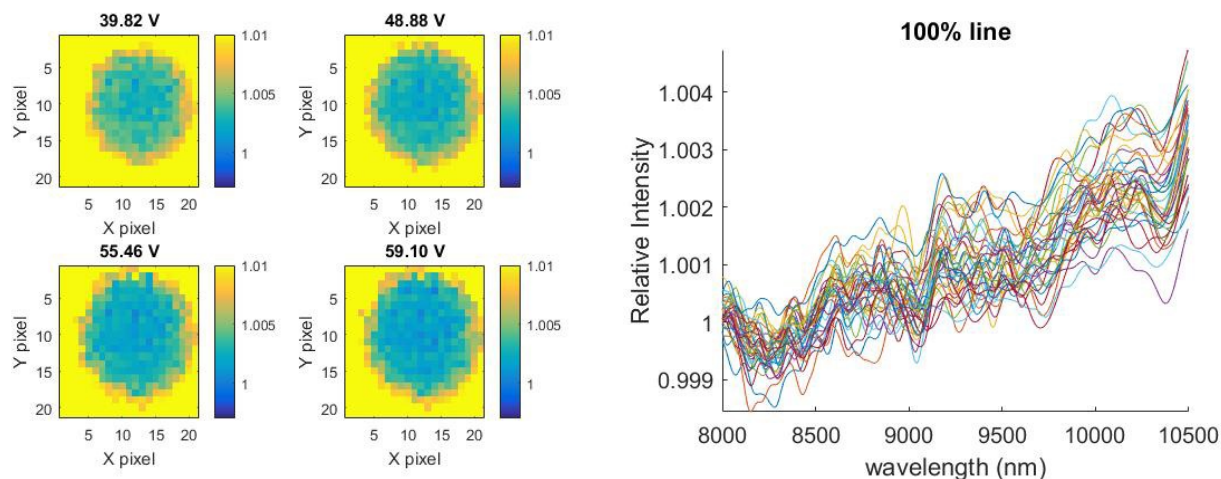


Figure 7. SNR measurements by the 100% line method on gold mirror. Left: Relative intensity signal of the image at four FPI actuation voltages. Right: Relative intensity signal over the full spectral range of 36 different pixels. We noticed a drift the environment temperature.

The system's spectral accuracy was tested by measuring a transmission hyperspectral image of a polystyrene calibration foil. This sample is a good candidate for spectral calibration because it has narrow band spectral features within the range of interest. The source used is an 8 inch blackbody target set to 373K and covering the entire field of view. In Figure 8, the measured relative transmission is shown for four different actuation voltages applied to the interferometer. As expected, we observed ring-like patterns in the raw data images corresponding to the maximum transmission wavelength frequency shift which increases with distance from the optical axis. On the right-hand side of Figure 8, the transmission spectra measured on the 36 center pixels over the full spectral range of the image are presented. The spectral sampling pitch for these measurements is 25 nm. Wavelength correction (see section 2.3 above) is applied to the spectral dimension of the datacube which leads to spectra, exhibiting features at the same wavelength and with very similar amplitudes for all 36 pixels. This confirms the efficiency of the correction of the spectral shift introduced by the incidence angle distribution on the FPI. For comparison with an FTIR spectrometer, the red dashed line on the graph is the spectrum obtained by convoluting the FPI transfer function with a spectrum of the same polystyrene foil measured in transmission with a FTIR, Vertex spectrometer from Bruker. This spectrometer is used with a sampling resolution of 4 cm^{-1} to calibrate the wavelengths of MICROXCAM-384i-HS. We believe that the slight discrepancies in the peak

positions between the spectra are due to the inaccuracy of the convolution. Effectively, the transfer functions used for the convolution are approximate functions of the actual transmission bands of the FPI.

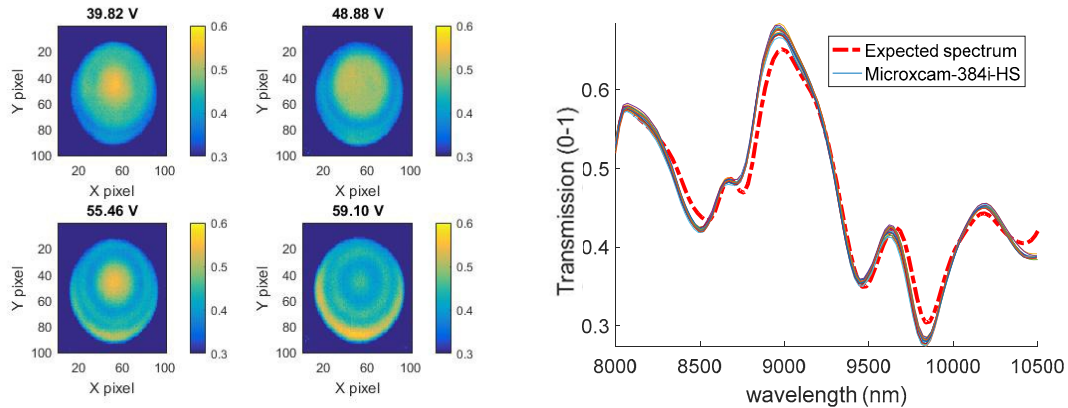


Figure 8. Image acquired at 4 different wavelengths (left) and transmittance spectra (right) of a polystyrene calibration sample. In the graph are superimposed the spectra obtained for the 36 pixels located at the center of the images, to evidence the good response uniformity and the validity of the correction of the wavelength shift due to the incidence angle on the FPI. The red dashed line is the spectrum obtained by convoluting the FPI transfer function with the spectrum of the same polystyrene foil measured with the Vertex FTIR spectrometer at a resolution of 4 cm^{-1} resolution.

4. HYPERSPECTRAL IMAGING TEST RESULTS

4.1 Transflectance IR hyperspectral imaging

Infrared imaging spectroscopy can be a fast and easy technique for detection and identification of adulterants in different products. As an example, samples of maple syrup, corn syrup and molasses were measured with our hyperspectral camera and basic spectroscopic analysis was subsequently performed. As presented in the visible image of Figure 10C, the components were spread with a cotton swab directly from their commercial bottles over a gold reflective surface. As no additional sample preparation was performed, the thickness was non uniform. A transflectance hyperspectral datacube was acquired for the three samples simultaneously in the configuration shown in Figure 9.

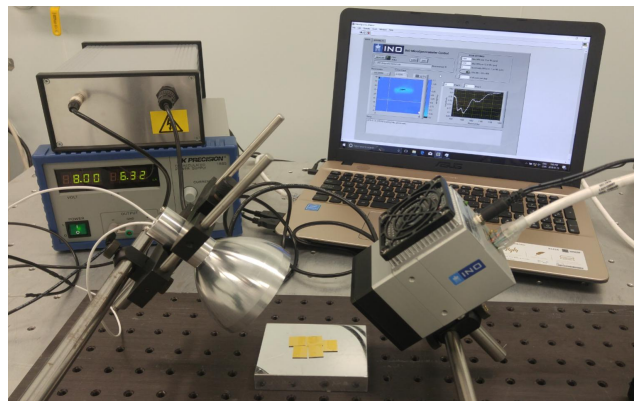


Figure 9. Transflectance hyperspectral imaging setup. The IR source is a 70W glabar inside a 3-inch diameter parabolic mirror (Hawkeye Technologies).

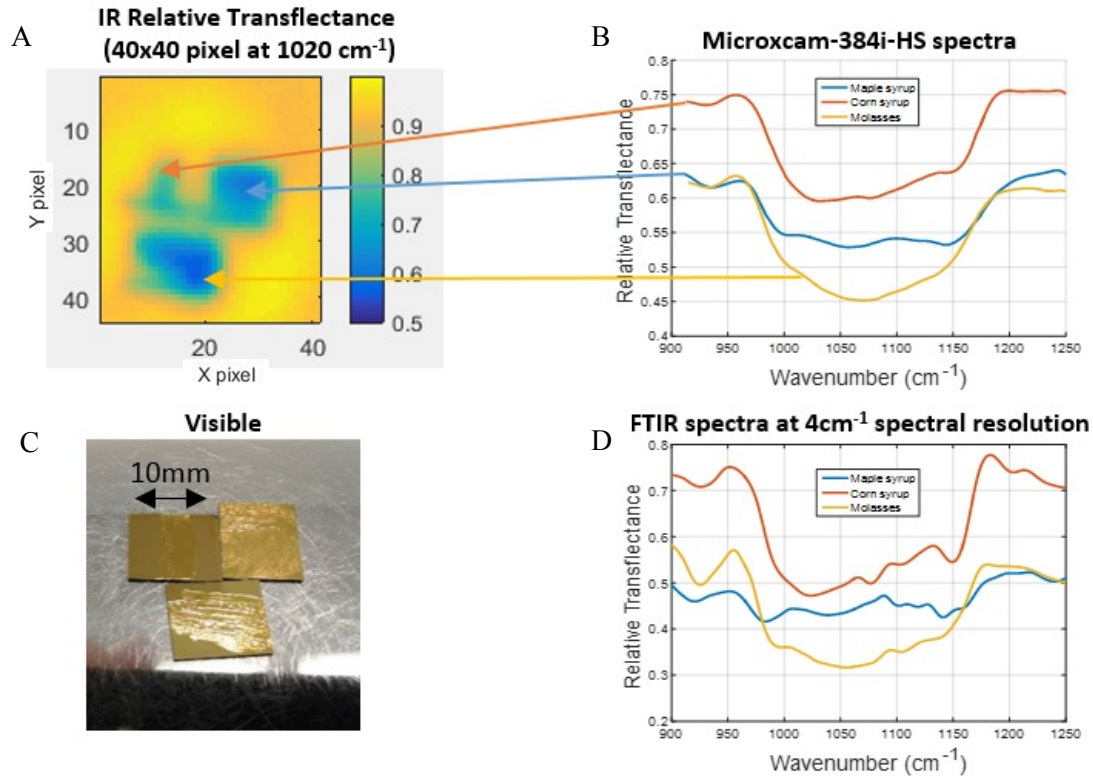
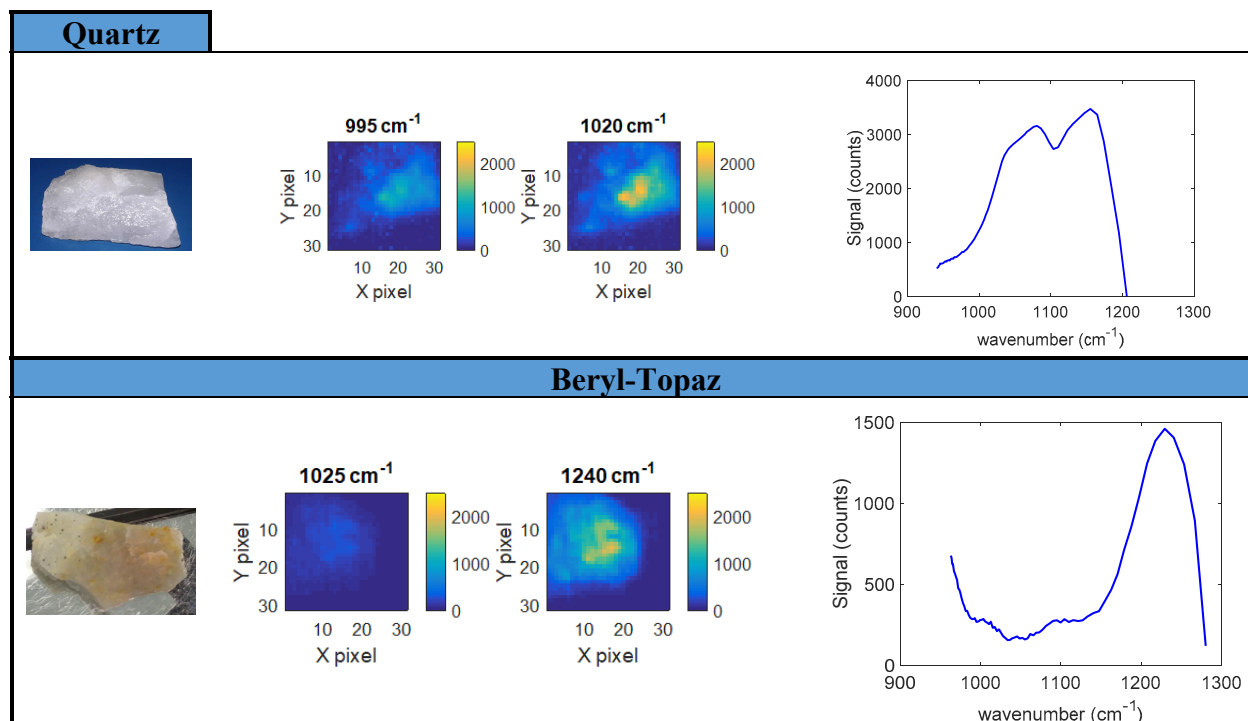


Figure 10. Simultaneous IR spectral transfectance imaging of maple syrup, corn syrup and molasses.

The spectra on Figure 10B are the unprocessed transfectance data of one pixel for each syrup. There are noticeable differences in the three syrups spectral signatures. Variations on the absolute relative transfectance inside an image are due to the sample's non-uniform thickness. However, the spectral signature is the same for every pixel of each syrup. Figure 10D shows spectra of the same samples obtained with the Vextex FTIR spectrometer at 4 cm^{-1} resolution. These spectra confirm the presence of the spectral features observed with MICROXCAM-384i-HS. The instrument could be used to identify syrup mixtures and quantify their concentrations with the help of custom spectroscopy analysis algorithms and of a reference spectra library.

Spectral signatures of different rock samples were also measured to evaluate the instrument's potential for mineral spectroscopy applications. The spectra are shown in Table 3 for quartz and beryl-topaz samples.

Table 3. Visible image, spectral images and reflection spectra of quartz and beryl-topaz samples obtained with MICROXCAM-384i-HS



5. CONCLUSIONS

We developed a portable fingerprint region hyperspectral imager, MICROXCAM-384i-HS, based on a MEMS FPI interferometer and a broadband microbolometric detector array. The accuracy of the correction of the spectral shift due to the incidence angle distribution on the FPI was verified by measurements with a commercial FTIR spectrometer. The performances of the LWIR hyperspectral camera were measured in terms of spectral resolution, tunability, response time, NESR and spatial resolution. LWIR imaging spectroscopy measurements were performed with MICROXCAM-384i-HS to demonstrate its abilities for detection and identification of different products. The camera is available as a development kit, intended for customers who wish to develop new applications inside and outside the laboratory. It includes driver electronics and data acquisition software to ease its use. Work is currently underway to further reduce response time and improve spatial resolution

REFERENCES

- [1] Jerominek, H., Pope, T.D., Alain, C., Picard, F., Fuchs, R.W., Lehoux, M., Zhang, R., Grenier, C., Rouleau, Y., Cayer, F., Savard, S., Bilodeau, G., Couillard, J.-F. and Larouche, C., "128x128 pixel uncooled bolometric FPA for IR detection and imaging," Proc. SPIE 3436, 585-592 (1998).

- [2] Chevalier, C. et al., "Introducing a 384x288 pixel terahertz camera core", Proc. of SPIE, Vol. 8624, art.no. 86240F, 2013.
- [3] Fisette, B., Tremblay, M., Oulachgar, H., Généreux, F., Béland, D., Beaupré, P., Julien, C., Gay, D., Deshaies, S., Terroux, M., Tremblay, B., Dufour, D. and Alain, C., "Novel vacuum packaged 384x288 broadband bolometer FPA with enhanced absorption in 3-14um wavelength range" Proc. SPIE 10177, 10177R, 2017.
- [4] Terroux, M., Marchese, L., Dufour, D., Pancrati, O., Doucet, M., Blanchard, N., Bergeron, A., "Millimeter/submillimeter wave video imaging using a THz camera for outdoor conditions", International Conference on Infrared, Millimeter, and Terahertz Waves, IRMMW-THz, art. no. 7758822, 2016.
- [5] Garcia-Blanco, S., Topart, P., Desroches, Y., Caron, J.S., Williamson, F., Alain, C., Pope, T. and Jerominek, H. "Low-temperature vacuum hermetic wafer-level package for uncooled microbolometer FPAs" Proc. SPIE 6884, 68840P1-68840P8 (2008).
- [6] Ebermann, M., Neumann, N., Hiller, K., Gittler, E., Meinig, M., Kurth, S. "Recent advances in expanding the spectral range of MEMS Fabry-Perot filters", Proc. SPIE 7594, MOEMS and Miniaturized Systems IX, 75940V (18 February 2010).